42nd AIAA Aerospace Science Meeting and Exhibit
5-8 January 2004, Reno, Nevada

AIAA 2004-411

ROLE OF DROPLET DISTORTION AND BREAK-UP IN LARGE DROPLET AIRCRAFT ICING

Geoffrey Luxford, David W. Hammond and Paul Ivey
The School of Engineering, Cranfield University,
Cranfield, Bedfordshire, MK43 0AL, UK

ABSTRACT

Experimental and analytical evidence is presented to illustrate droplet distortion and potential break-up in the flow conditions similar those of a drizzle droplet in the vicinity of an aerofoil. The droplet size range considered is 100μm to 500μm. The current research is at ambient temperature but with equivalent parametric conditions to SLD icing. While the results support the contention that smaller droplets, <100μm, remain essentially spherical, the larger droplets become sufficiently distorted to affect their drag characteristics and can break up due to the transient aerodynamic forces.

NOMENCLATURE

CCD	Charge Coupled Detector
LED	Light emitting diode
SLD	Supercooled Large Droplets
SLR	Single Lens Reflex
VED	Volume Equivalent Diameter
D	Droplet diameter
R	Aerofoil leading edge radius
U	Velocity, or velocity difference
F	Drag force on droplet
T_t	Nominal Droplet transit time, $= R/U_a$
T_d	Droplet oscillation period, $= (\pi/4).\sqrt{(\rho_d.D^3/\sigma)}$
a	Droplet acceleration
ρ	Fluid density
μ	Fluid viscosity
σ	Surface tension
$_a$	Subscript for air
$_d$	Subscript for droplet

Re	$= \rho.U.D/\mu$	Reynolds number
We	$= \rho.U^2.D/\sigma$	Weber number
Bo	$= \rho_d.a.D^2/\sigma$	Bond number
Cd	$= F/(\pi.D^2.\rho.U^2/8)$	Drag coefficient
Oh	$= \mu/\sqrt{(\rho.\sigma.D)}$	Ohnesorge No.
Oh_a	$= We^{0.5}/Re$	
D/R		Length scaling ratio
ρ_d/ρ_a		Density ratio
μ_d/μ_a		Viscosity ratio

Unless otherwise stated, the droplet Reynolds number and Weber number use the VED, velocity differential between droplet and air and the local air properties.

INTRODUCTION

It has been found that conditions of freezing drizzle, with larger supercooled water droplets, 100μm to 500μm VED, can result in excessive icing of an aircraft wing. This icing with Supercooled Large Droplets, or SLD icing, can be an appreciable hazard in that it can form aft of the ice protection to degrade the performance of the wing and control surfaces.

These larger droplet diameters behave differently to the more familiar Cloud Icing droplets, < 100μm VED, in that surface tension is less dominant in maintaining shape and integrity against the aerodynamic pressure. Also the dynamic response times, and/or residence times, become substantially longer.

The issue considered is the effect on such droplets as they penetrate the flow field around the leading edge of an aerofoil. In comparison to the surface tension forces and their dynamic response time, droplets experience a strong transient aerodynamic force. These forces can be of sufficient magnitude and appropriate duration to cause substantial distortion and possible break-up of the droplets. The distortion can affect the droplet velocity and trajectory due to the increased air drag, which can then affect the distribution, velocity and orientation of droplet impact with the aerofoil.

Much of the previous droplet research[1 to 10] concerned with droplet distortion and break-up has been with diameters of several mm, whereas this research is concerned with droplets of a fraction of a mm diameter. While in some respects this difference in droplet scale can be allowed for, the scaling rules may not adequately account for important differences. This can only be achieved by working with the actual scale of droplets, resulting in some significant practical difficulties, which this research attempts to address.

Various experimental, theoretical and modelling capabilities are and have been developed to investigate the distortion and break-up of these smaller droplets. These are presented and considered, together with some preliminary results and conclusions.

SCALING ISSUES & PARAMETERS

An important issue is the effect of spatial and temporal scaling. In this the various scaling parameters are considered. These can be classified into two groups,

1. Steady state
2. Transient and Dynamic

Steady State effects

In many respects the response of a droplet depends only on the magnitude of the forces applied. This is particularly so for equilibrium conditions where changes occur reasonably slowly.

It such conditions, where heat and mass exchange are negligible, the droplet conditions are adequately described by the Weber number, which represents the ratio of the pressure force to the surface tension force, and Reynolds numbers, which represents the ratio of pressure force to viscous force.

The aerodynamic pressure force on a droplet travelling through air is balanced against the acceleration forces of the droplet mass. This produces a non-uniform pressure across the surface interface which is accommodated by surface tension and variations in surface curvature. As a result the droplet distorts and when the conditions are severe enough it will break-up, mostly as determined by the Weber number.

The aerodynamic force and drag coefficient will be modified by the Reynolds number in conjunction with the droplet distortion. This makes the droplet more oblate and increases its outer diameter. The Weber, Reynolds and Drag coefficient are normally based on the VED, which is assumed to be constant.

It can be shown, by combining parameters, that the acceleration of the droplet is related to the Drag coefficient and Weber number through the relationship;

$$Bo = (3/16).Cd.\,We \qquad (1)$$

For the conditions of interest and a spherical droplet the drag coefficient is between 0.4 and 0.5. Relative to the outer diameter of a distorted droplet the drag coefficient increases as the droplet becomes more oblate, with an upper limit of 1.0 for a flat disc.

In experimental measurements, the droplet distortion may not be known, so the parameter groups must then be related to the VED, rather than the actual outer diameter of the distorted droplet.

The Ohnesorge number, Oh, can either be related to the droplet properties, or the local air properties. The value of this parameter is to eliminate velocity. With the air properties this can be derived from the Weber number and Reynolds number as;

$$Oh_a = We^{0.5}/Re = \mu_a/(\rho_a.\sigma.D)^{0.5} \qquad (2)$$

The significance of this is that in relation to distortion and break-up the Weber number will have a particular value range. Hence for a given surface tension and air properties it can be shown that the Reynolds number will be proportional to the square root of droplet size.

For a free falling droplet of around 5mm diameter the Reynolds number is around 4000. This is about 20 times larger than droplets relevant to SLD icing, for which the Reynolds number will be around 700. Within this Reynolds number range the drag coefficient, for a spherical drop, varies by about 20%. While this variation is moderate, there can be a different pressure distribution with the change in Reynolds number. This could affect the droplet distortion and hence its drag and break-up characteristics.

A basic analysis of the relevant forces[5] indicates that droplet break-up can occur at;

$$Cd.\,We = 8 \quad \text{or} \quad Bo = 1.5 \qquad (3)$$

Wierzba[2] indicated break-up is only likely to occur for similar condition, $12 < We < 13$, when the aerodynamic force is suddenly applied, in which case the dynamic response of the droplet contributes significantly to the break-up. Liu[3] indicates that for a steady aerodynamic load the critical Weber number, for a free-falling droplet, is around 20 to 22.

For typical SLD conditions in the flow field around an aerofoil it would seem that the droplet Weber number can result in substantial droplet distortion and possibly well exceed the critical value for break-up.

There are two factors which may moderate this;

(1) The deceleration of droplets to stay within the critical limits.

(2) The limited time available before impact with the aerofoil.

The droplet deceleration is considered later.

Transient effects

As a droplet traverses the flow field near an aerofoil it experiences a rapidly increasing aerodynamic force. In such transient conditions the droplet behaviour will depend on the time it takes to respond to such a force.

If the transit time is short, compared to the droplet response time, there will be little time to respond and it can remain intact against a much stronger aerodynamics force, possibly with little distortion.

If the transit time is similar to the droplet response time then the droplet will be substantially more sensitive to the force and so would distort and possibly break-up with a much lower aerodynamic force.

If the transit time is long compared to the droplet response time then the load will be more constant, so the droplet will have time to adapt. Also the droplet will have time to decelerate and so not experience such a strong aerodynamic force.

These transient loading conditions can be represented as a force pulse with a sloping front of duration t and amplitude 'We', as shown in Figure 1.

The resulting tolerance, in terms of Weber number, is shown as the conceptual graph in Figure 1 against the duration of the pulse.

Given the necessary magnitude and appropriate dura-

tion this could cause the droplet to break-up prior to impact with the aerofoil, which could significantly effect the SLD icing process.

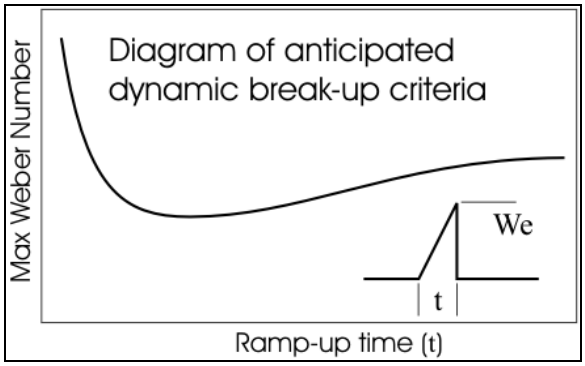

Figure 1

The transient ramp-up time for the droplet loading will be related to its transit time through the flow field. This will be of the order of $T_t = R/U_a$, where U_a is the free stream velocity. The droplet response time will be related to its vibration period, T_d.

Taking the ratio of these two times we obtain;

$$T_d / T_t = (\pi/4).[(D/R).\sqrt{((\rho_d/\rho_a).We_{nom})}] \quad (4)$$

Where We_{nom} is the nominal droplet Weber number for the free stream air velocity.

For relevant droplet conditions the Weber number and density ratio will remain about the same. Hence the primary variable factor in this is the ratio of the droplet diameter to the leading edge radius.

The implication is that SLD icing tests carried on a small scale model will not subject the droplets to the same transient conditions as they would experience with a full size aerofoil. Hence scale model tests may not satisfactorily reproduce full scale SLD icing and this issue needs to be considered in such tests.

SIMULATION AND MODELLING

A numerical simulation of the droplet motion dynamics has been developed. This calculates the trajectories and velocities of droplets for a given flow field. This is mostly used for the analysis of droplet motion in convergent wind tunnels, but can also be used for external flow where the flow field can be adequately described, such as the upstream flow around a cylinder, or for some simpler aerofoils[11, 12].

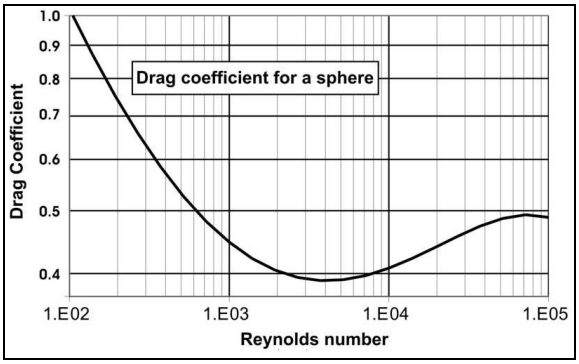

Figure 2

For spherical droplets the acceleration can be computed from the standard drag data[6] of Figure 2.

Where the Weber number is high enough, the drag increases due to droplet distortion. The correction used is shown in Figure 3.

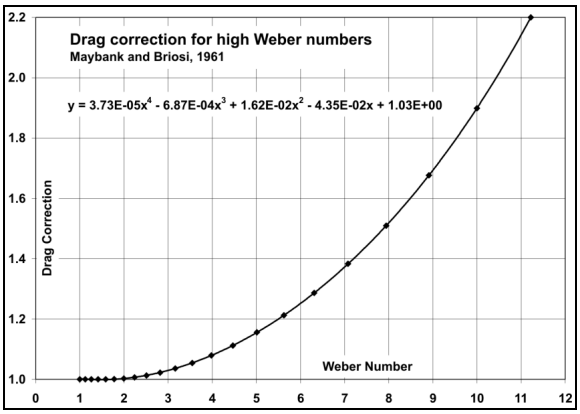

Figure 3

This data was for larger droplets and solid spheres of equal density and VED free-falling in atmospheric air and standard gravity[4]. While not exact, possibly due to a mismatch in Reynolds number, preliminary experimental results show an error of less than 15%.

Hence the simulation computes the droplet drag for a sphere of the same VED and Reynolds number. The drag correction for droplet distortion is then applied for the Weber number. This gives the relationship;

$$Cd = f(Re).g(We) \quad (5)$$

Where f(Re) and g(We) are the function relationships given in figures 2 and 3 respectively.

Droplet in the vicinity of a cylinder

Using equation (5) the transient forces were calculated, in terms of Weber number, as the droplet approaches the upstream stagnation zone of various size cylinders. This was to approximate the conditions near the leading edge of an aerofoil for a 200µm droplet in a free stream velocity of 100m/s. In this the droplet shape was assumed to instantaneously adapt

to the changing Weber number, which in practice may not happen, as considered in this evaluation.

The results of this analysis are shown in Figure 4. The nominal Weber number for the free stream velocity was about 33.

The cylinder radii considered were 10mm to 500mm. The periodic time for the droplet oscillation was about 0.26ms, as shown in Table 1.

Table 1; Effect of droplet size on vibration period

Diameter, µm	50	100	200	400
Period time, µs	33	92	261	737

It can be seen that for the 10mm and 20mm radius cylinders the rise time of the Weber number was substantially less than the periodic time of the droplet, so it is anticipated that the droplet could penetrate this flowfield without break-up, possibly without significant distortion, even thought the maximum Weber number was well above the critical value.

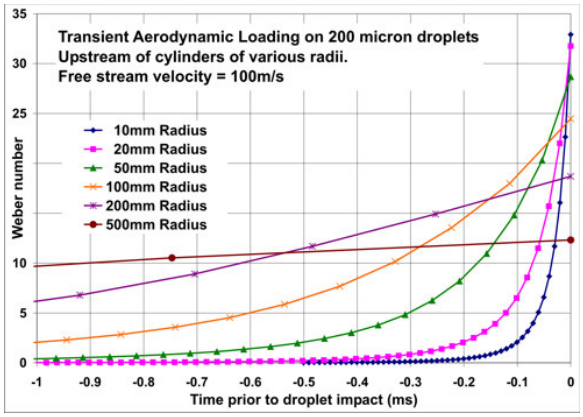

Figure 4; Droplet loading upstream of a cylinder

For the 50mm and 100mm radius cylinders the Weber number rise time is comparable with the droplet response time and the maximum Weber number sufficient to cause break-up for these transient conditions.

For the 200mm and 500mm radius cylinders the Weber number rise time is much longer than the response time of the droplet. The maximum Weber number is not of sufficient to otherwise cause break-up.

This indicates that for the conditions considered the droplet break-up is likely to occur for a leading edge radius of around 50mm to 100mm, which is understood to be typical for medium size passenger aircraft.

For a 10mm to 20mm leading edge radius of a scale model it appears that the droplets will not break-up.

It would thus seem that pre-impact break-up can be a significant issue in SLD icing of full-scale aircraft which is not reflected in scale model testing.

EXPERIMENTAL FACILITIES

To experimentally investigate the dynamic behaviour of droplets various experimental facilities have been developed. There are three parts to this;

1. Droplet conditioning
2. Measurement of droplet motion
3. Visualisation of droplets

Droplet Conditioning

This includes the small open-circuit convergent wind tunnel shown in Figure 5.

The inlet on the right is through a fibre screen into the plenum chamber box. On the left is the air diffuser connected to the external suction fan, shown in the inset. The tunnel is the 520mm long convergent transparent section, of about 300mm square at its inlet and about 75mm square at its outlet.

The maximum air velocity, about Mach 0.5, and test rig size where chosen to keep compressibility effects, costs and timescale within acceptable limits.

Figure 5; Convergent Wind Tunnel

The purpose of the tunnel is to subject water droplets, in the size range of interest to SLD icing, to sufficient aerodynamic force to result in substantial distortion and break-up.

In the vicinity of an aerofoil droplets experience decelerating and curvilinear flow, which is difficult to reproduce to scale in a small facility. It is much simpler to achieve similar conditions with an accelerating flow in a small convergent tunnel. Because the droplet then experiences decreasing air density this results in a small mismatch of the variation of droplet Reynolds number, which is currently neglected.

The numerical simulation for the droplet dynamics can be programmed to achieve a given variation in droplet loading, such as Weber number, and then determine the contraction profile to achieve this.

Using available data for droplet drag, Figure 2 & 3, the tunnel was designed to give a linearly increasing Weber number with time, as shown in Figure 6. The other two curves in this show the velocity for the droplet and air.

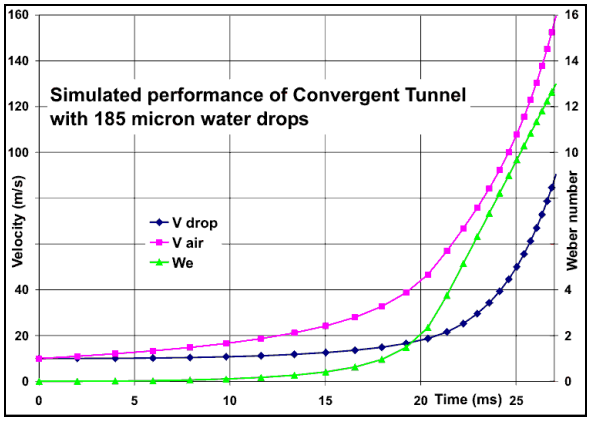

Figure 6; Tunnel Design Characteristics

In the current design the rise time for the Weber number is around 7ms for a 185µm droplet. This is much longer than the droplet dynamic response time, hence for initial experiments the droplets will experience near quasi-static conditions. For later experiments the tunnel contraction will be redesigned to produce more transient conditions that better represent the transient conditions near an aerofoil.

Droplet Generator

For the experiments it is necessary to have a source of droplets of known size. These are produced by a mono-dispersed droplet generator, shown in Figure 7. The actual droplet generator is 10mm diameter by 27mm long on the left-hand end. The larger part on the right-hand end is a pipe adaptor for the water feed into the back end of the generator.

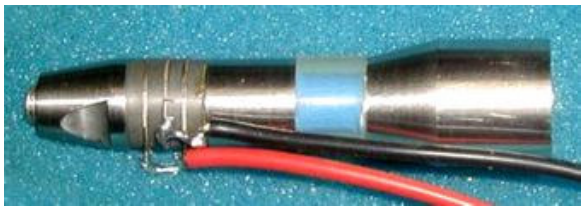

Figure 7; The droplet generator.

Pressurised water is forced through a small platinum nozzle at the left-hand end to produce a laminar water jet of controlled velocity and diameter. At the same time an alternating voltage is applied to piezoelectric rings around the centre section, which introduces a small vibration to the nozzle at the required frequency. This causes the jet to break-up up as shown in Figure 8, which produce a uniform stream of droplets once the vibrations decay, as shown in Figure 9.

Figure 8; Droplets being formed from a jet.

The droplets in Figure 9 are about 270µm diameter, with a velocity of about 10m/s, left to right, at a frequency of about 15kHz and pitch of about 0.7mm. The small irregularity in droplet spacing is caused by an aerodynamic interaction between them.

Figure 9; Droplet stream from Drop Generator

The droplets are then injected into the accelerating airflow of the convergent tunnel, where they are subjected to strong aerodynamic forces so the resulting effects can be investigated.

Measurement of droplet Velocity and Acceleration

One objective is to determine the drag characteristics of these small droplets when distorted by aerodynamic forces. Most current data is for free falling droplets 20 times bigger in atmospheric conditions. The Reynolds number straddles laminar and turbulent condition, so this could affect the droplets behaviour.

The critical issue is to experimentally determine the drag-coefficient of the droplets for known conditions of Reynolds number and Weber number with an adequate degree of accuracy. Given droplets of known diameter and mass, the drag-coefficient can then be determined from the droplet acceleration.

With free falling droplets the acceleration force is known to be 1g. For these experimental conditions the droplet acceleration is typically 500g. This has to be determined with the droplets travelling at a substantial velocity, typically 30 to 50m/s.

The method for determining the droplet acceleration is shown in Figure 10. A droplet intercepts three equispaced, parallel, coplanar laser beams. This produces electrical pulses from high-speed photo detectors the other side of the transparent tunnel. The time intervals between the resulting pulses are then used to determine the droplet velocity and acceleration.

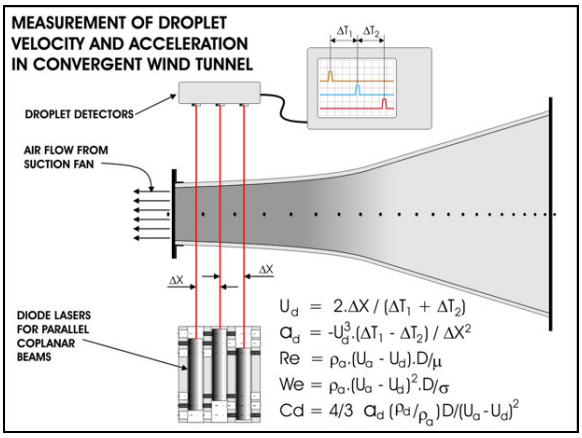

Figure 10; Droplet Measurement Method

This is achieved by double differencing the interruption timings of the laser beams. Such a procedure is

notorious for introducing large errors as it involve small differences between relatively large values. When this process is repeated twice any initial errors are greatly magnified. To ensure adequate accurate various precautions were taken to minimise the errors.

An error analysis showed that a laser beam spacing of 25mm and timing accuracy of 1µs would be acceptable. In this it was found that the most critical issue was the symmetry of the laser beam spacing. It was found difficult to ensure this by direct calibration, so as a precaution the diode lasers were mounted in an aluminium block, which could be inverted, as shown in figure 11, to reverse any asymmetry.

Figure 11

Averaging the measurements taken with the block in the normal and inverted position then cancelled errors due to any spacing asymmetry in the laser beams.

Four measurements for the same conditions gave an average velocity of 30.67m/s and acceleration of 4404m/s^2 for 273µm droplets. The velocity and acceleration variance was 0.7% and 4.7% respectively.

This experimental result for droplet velocity and acceleration are plotted in Figure 12 together with the simulated results for the same conditions.

The simulated result for the same location and conditions, with distortion correction, was 31.26m/s and 3824m/s^2 respectively. The average discrepancy was 2% and 15% respectively. In practice the acceleration error was 11% after allowing for the velocity error.

These results were with a Weber and Reynolds number of about 7.6 and 700 respectively. From figure 3 this gives a distortion drag correction of about 1.45.

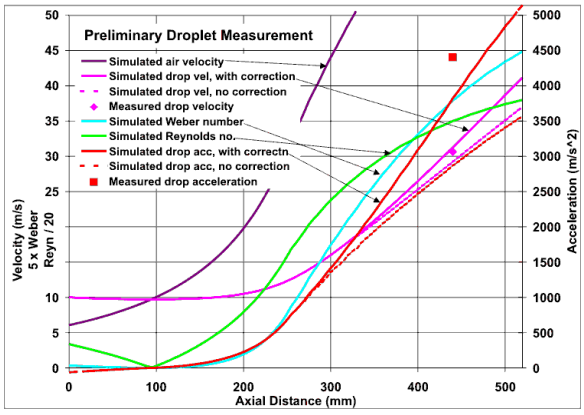

Figure 12; Preliminary Droplet Measurement.

Without the distortion correction the simulated droplet velocity at the same location was 29.19m/s and the acceleration 2866m/s^2. This gave discrepancies of 5% for velocity and 54% for acceleration. The effect on velocity is quite small due to the short time for the acceleration discrepancies to accumulate.

The acceleration result indicates that while there may be errors in the drag calculation extrapolated from free-falling droplets, these were very much less than not applying any distortion drag correction at all.

Further acceleration measurements and analysis is anticipated to improved drag correction data for distorted droplets at lower Reynolds numbers.

Visualisation of droplets

As well as measuring the behaviour of droplet distortion and break-up, it is also necessary to obtain images to provide further data. Because of the small droplet size, down to 100µm, and high velocity, up to 100m/s, this involves substantial technical difficulty.

The high-speed cameras systems normally used for such imaging are expensive, £50k to £250k. The preliminary imaging system is shown in Figure 13.

In this a CCD still camera was used to obtain the images. The droplets were back illuminated by a pulsed LED. Such devices are now available with much higher intensities than was previously possible.

A conventional SLR digital camera could be used, but at a CCD astronomical camera is currently used because of its lower background noise. This allows imaging with the substantially lower light levels from the LED flash, compared to that from a pulsed laser. Further development of the LED flash unit is expected to substantially improve its output.

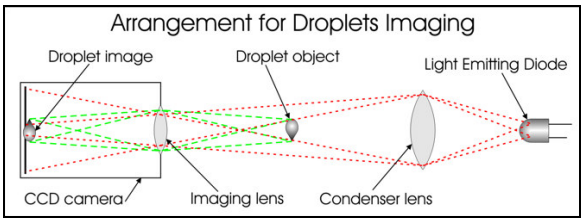

Figure 13

Figure 14 shows an image obtained with droplets down to 270µm diameter with a velocity of around 10m/s. This shows the coalescence of droplets, which can affect acceleration measurements. This is being investigated to minimise such coalescence.

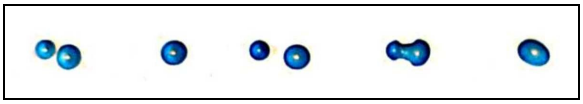

Figure 14; Coalescence from droplet interaction.

Figure 15 shows a preliminary image of droplets distorted by aerodynamic force. These have estimated

VEDs of 300 to 350μm and velocity of around 25m/s.

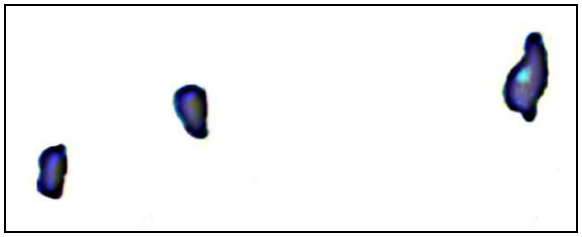

Figure 15; Aerodynamic droplet distortion.

The droplet conditioning and imaging needs improving to obtain better measurement and imaging, however Figure 15 indicates the extent of droplet distortion for typical SLD aerodynamic conditions.

FURTHER DROPLET MODELLING PLANNED

Further anticipated droplet modelling will take various forms;

1. Images of distorted droplets will be used to determine the pressure distribution and drag;
    a. by use of CFD modelling with the prescribed droplet geometry.
    b. from the pressure differential across the droplet surface, deduced from its curvature and surface tension.
2. Simplified dynamic droplet models will be developed and tested to see if they can be used to predict transient aerodynamic distortion and break-up criteria.

CONCLUSIONS

With respect to the potential break-up of droplets in the vicinity of an aerofoil, it would appear that this is quite feasible in conditions relevant to SLD icing of full size aircraft with relevant combinations of droplet size and aerofoil scale.

With respect to the distortion and drag of droplets the preliminary experimental result indicates that the extrapolation from free falling droplet gives a reasonable quasi-static approximation for droplets relevant to SLD conditions, but further data is required.

Current data and analysis indicates that the motion, velocity and orientation of droplets can be substantial affected by distortion due to aerodynamic forces in the vicinity of a full scale aerofoil and this could significantly affect their impact with the aerofoil.

It would appear that with SLD icing the dynamic response of droplets, in terms of distortion, motion, velocity and break-up, is likely to be different in scale model testing, in comparison to full size aircraft. As a result this may require appropriate allowance for these issue in testing and modelling these processes.

Preliminary droplet imaging has been achieved with low-cost facilities, using flash lighting from a high intensity pulsed LED. Further development is required to increase the intensity and image quality. These images show that droplets will distort and break-up in conditions relevant to SLD icing.

Calibrated monodispersed droplets of a wide range of sizes can be produced from the droplet generator, but further developments are required to reduce coalescence of these droplets in the wind tunnel.

ACKNOWLEDGEMENTS

Thank to Paul Spooner of the CAA for guidance, support and sponsorship of this research. Thanks to Tom Bond and Dean Miller at NASA for their help, advice and support. Thanks to Cranfield University, its staff and workshop for providing and constructing the necessary facilities. Thanks to Prof Chris Freeman for his help and advice in this research. Thanks to Linx inkjet printers for their help and supplies. Thanks to ADINA Research for provision of CFD facilities. Thanks to everyone else who have provided help, advice and support for this research.

REFERENCES AND BIBLIOGRAPHY

1. O. A. Basaran, 1992, "Nonlinear oscillation of viscous liquid drops", J. Fluid Mech. V241, pp. 169-198
2. A. Wierzba, 1990, "Deformation and break-up of liquid drops in a gas stream at nearly critical Weber numbers", Exp in Fluids 9, 59-64.
3. H. Liu, 2000, "Science an Engineering of Droplets, fundamentals and applications", Noyes publications.
4. J. Maybank & G.K. Briosi, 1961, "A Vertical Wind Tunnel", Suffield Technical Paper No. 202, DRB project no.D52-95-10-07.
5. A. Frohn and N. Roth, 2000, "Dynamics of Droplets", Springer Verlag.
6. Massey, 1970, "Mechanics of Fluids", Van Nostrand 2nd Edition.
7. R. Clift, J.R. Grace, M.E. Weber, 1978, "Bubbles, Drops & Particles", Academic.
8. R. Schmehl, 2002, "Advanced Modelling of Droplets Deformation and Break-up for CFD Analysis of Mixture Preparation", ILASS-Europe.
9. R.P. Chhabra and D. De Kee, 1992, "Transport Processes in Bubbles, Drops and Particles", Hemisphere Publishing.
10. S. Middleman, 1995, "Modelling Axisymmetric Flows", Academic Press.
11. I.H. Abbot and A.E. Doenhoff, 1959, "Theory of Wing Sections", Dover
12. H. Kober, 1952, "Dictionary of Conformal Presentations", Dover.